

Electrical conductance of two-dimensional random percolating networks based on mixtures of nanowires and nanorings: A mean-field approach along with computer simulation

Yuri Yu. Tarasevich^{*} and Andrei V. Eserkepov[†]

Laboratory of Mathematical Modeling, Astrakhan State University, Astrakhan 414056, Russia



(Received 9 January 2023; accepted 17 February 2023; published 6 March 2023)

We have studied the electrical conductance of two-dimensional (2D) random percolating networks of zero-width metallic nanowires (a mixture of rings and sticks). We took into account the nanowire resistance per unit length and the junction (nanowire-nanowire contact) resistance. Using a mean-field approximation (MFA) approach, we derived the total electrical conductance of these nanowire-based networks as a function of their geometrical and physical parameters. The MFA predictions have been confirmed by our Monte Carlo (MC) numerical simulations. The MC simulations were focused on the case when the circumferences of the rings and the lengths of the wires were equal. In this case, the electrical conductance of the network was found to be almost insensitive to the relative proportions of the rings and sticks, provided that the wire resistance and the junction resistance were equal. When the junction resistance dominated over the wire resistance, a linear dependency of the electrical conductance of the network on the proportions of the rings and sticks was observed.

DOI: [10.1103/PhysRevE.107.034105](https://doi.org/10.1103/PhysRevE.107.034105)

I. INTRODUCTION

Transparent conductive electrodes are an essential component of smart electronics and optoelectronics, such as smart windows, touch panels, and solar cells. Metal nanowire-based transparent conductive electrodes (TCEs), such as Cu, Ag, and Au nanowire electrodes, are considered to be a new generation of TCEs that are capable of replacing indium tin oxide-based electrodes [1].

Nanoring-based TCEs are a promising kind of TCE. Different methods exist for synthesizing metallic nanoring-based TCEs. However, in all cases, any TCE includes both nanorings (NRs) and nanowires (NWs). The latter may be bent or wavy. The fraction of NWs and NRs may vary. Table I presents some published data on synthesized metallic nanorings.

Notice that for cylindrical wires of an isotropic metal, the electrical resistivity depends on the wire diameter, tending to the value of the bulk resistivity as the wire diameter increases [10]. Some experimental data are collected in Table II. For comparison, the electrical resistivity of bulk silver is $15.9 \text{ n}\Omega\text{m}$ [11]. The temperature dependence of the resistivity should also be borne in mind [10,12].

Selzer *et al.* [17] reported that a value of the resistance of a single Ag nanowire (mean diameter of 90 nm) is $4.96 \pm 0.18 \text{ }\Omega/\mu\text{m}$ (the values in the corresponding row in Table I were calculated using these data), while the junction resistance is $25.2 \pm 1.9 \text{ }\Omega$ (annealed junctions) and $529 \pm 239 \text{ }\Omega$ (nonannealed ones). For AgNWs (average diameter of $70 \pm 10 \text{ nm}$ and average length of $8 \pm 3 \text{ }\mu\text{m}$), Charvin *et al.* [19], knowing the experimental sample sheet resistance and expecting the simulated one to be the same, estimated the junction resistance as $14 \pm 2 \text{ }\Omega$. Gomes da Rocha *et al.* [16], comparing simulations with experimental data, reported estimates of

the junction resistance from $2.28 \text{ }\Omega$ to $152 \text{ }\Omega$ ($45 \pm 31 \text{ }\Omega$) (see the Supplemental files in Ref. [16]).

Monte Carlo (MC) simulations of the electrical conductance have been performed for random two-dimensional (2D) systems of conductive sticks [20–25] and rings [6,26,27]. The electrical properties of such systems have been considered theoretically using a percolation theory [28], a mean-field approximation (MFA) approach [6,21,24–27,29], network analysis [30,31], and an effective medium theory (EMT) approach [32].

MC simulations of electrical percolation in thin films with conductive disks and sticks have been performed [33]. The effective conductance of nanocomposites as a function of their relative concentrations has also been investigated. A synergistic effect has been reported when the disks and sticks combine properly. The widely used junction resistance dominant assumption (JDA) (see, e.g., Refs. [22,23,34,35]) has been used, i.e., both disks and sticks were assumed to have no electrical resistance, while a junction between any two conductive fillers was assumed to be a resistor. The resistance of a stick-stick junction was assumed to be five times larger than that of a disk-disk one since a contact between any two disks is an area, while a contact between any two sticks is a point contact. The dependencies of the electrical conductance with respect to the mass ratio of the disk to stick and to stick length have been plotted.

Recently, the MFA has been successfully applied to pure nanoring-based and to pure nanostick-based random, dense 2D systems [24–27]. However, here the MFA was applied to a mixture of conductive fillers having different shapes. The goal of the present study was the application of the MFA to 2D systems consisting of randomly deposited conductive NRs and nanosticks.

The rest of the paper is constructed as follows. Section II presents our computational and analytical methods, viz., Sec. II A describes some technical details of our

*Corresponding author: tarasevich@asu.edu.ru

†dantealigjery49@gmail.com

TABLE I. Published data on metallic nanorings.

Reference	Material	Ring diameter, μm	Wire diameter, nm
Zhou <i>et al.</i> [2]	Ag	4.8–20	≈ 165
Zhan <i>et al.</i> [3]	Cu	23	≈ 200
Yin <i>et al.</i> [4]	Cu	8–20	50
Azani and Hassanpour [5], Azani <i>et al.</i> [6]	Ag	15 ± 5	120 ± 20
Li <i>et al.</i> [7]	Ag	7.17–42.94	76
Feng <i>et al.</i> [8]	Ag	10	20–40
Ning <i>et al.</i> [9]	Ag	6.54–30.67	66.7–115.5

simulation and Sec. II B is devoted to an analytical consideration using a MFA. In Sec. III, we present our main results and compare the MFA predictions with computer simulations. Section IV summarizes the main results and suggests possible directions for further study.

II. METHODS

A. Simulation

Two kinds of conductive fillers were used in our simulation, viz., rings with a given radius r and equiprobably orientated zero-width sticks with a given length l . The electrical resistance per unit length of each filler was ρ_w .

The fillers of both kinds were randomly placed on an insulating substrate. Their centers were independently and identically distributed within a square domain of size $L \times L$. To reduce the finite-size effect, periodic boundary conditions (PBCs) were applied along both mutually perpendicular directions (Fig. 1). Let the number density of the sticks be

$$n_s = \frac{N_s}{L^2}, \quad (1)$$

while the number density of the rings is

$$n_r = \frac{N_r}{L^2}. \quad (2)$$

Since the electrical conductance is our primary interest, the total number density of fillers,

$$n = n_r + n_s, \quad (3)$$

was above the percolation threshold, $n \geq n_c$, in any case. For each value of the number density, simulations were performed for different proportions of rings and sticks. When the desired number density of the fillers was reached, the PBCs were removed, allowing us to consider the model as an insulating film of size $L \times L$ covered by conductive fillers. Then, superconductive busbars were attached to the opposite borders of the domain. A potential difference V_0 was applied to these busbars. The electrical resistance of each contact (junction) between any two fillers was R_j . The electrical resistance of each contact (junction) between a filler and a busbar was R_b . Both kinds of junctions were assumed to be ohmic. Consider a segment of the conductive filler (either a stick or a ring) between the two nearest junctions belonging to it. If a length of this segment is a , then its resistance is $R_s = \rho_w a$. Thus, a random resistor network (RRN) exists. This RRN is irregular with different branch resistances. Applying Ohm's law to each branch and Kirchhoff's point rule to each junction, a system of linear equations (SLEs) can be obtained. Although this SLE is huge, its matrix is sparse; therefore, numerical solution of

TABLE II. Published data on electrical resistivity of Ag nanowires, ordered in ascending order of nanowire diameter. We used original data on the electrical conductivity [13,14] to calculate the electrical resistivity. 2-P and 4-P are related to the two-point probes method and four-point probes method, respectively.

Reference	Method	T (K)	Length (μm)	Diameter d (nm)	ρ_w^* (n Ω m)
Bid <i>et al.</i> [10]	2-P	295	6	15	41.1
Bid <i>et al.</i> [10]	2-P	295	6	30	34.9
Bellew <i>et al.</i> [15]	4-P	room temp.	7 ± 2	42 ± 12	20.3 ± 0.5
Bid <i>et al.</i> [10]	2-P	295	6	50	29.2
Gomes da Rocha <i>et al.</i> [16]	4-P	room temp.	6.7	50 ± 13	22.6 ± 2.3
Zhao <i>et al.</i> [12]	2-P	room temp.	44	84	21.3
Selzer <i>et al.</i> [17]	4-P	room temp.	25	90	31.6 ± 1.2
Wang <i>et al.</i> [14]	4-P	room temp.	4.88	93.2	28.5
Wang <i>et al.</i> [14]	4-P	room temp.	14.67	97.0	32.9
Bid <i>et al.</i> [10]	2-P	295	6	100	27.8
Kojda <i>et al.</i> [13]	4-P	293	15 ± 1	120 ± 20	37 ± 13
Kojda <i>et al.</i> [13]	4-P	293	11 ± 1	107 ± 5	29 ± 5
Kojda <i>et al.</i> [13]	4-P	293	13 ± 1	140 ± 10	27 ± 6
Kojda <i>et al.</i> [13]	4-P	293	14 ± 1	150 ± 3	25.1 ± 1.3
Bid <i>et al.</i> [10]	2-P	295	6	200	23.3
Cheng <i>et al.</i> [18]	2-P	290	27.23	227	79.1

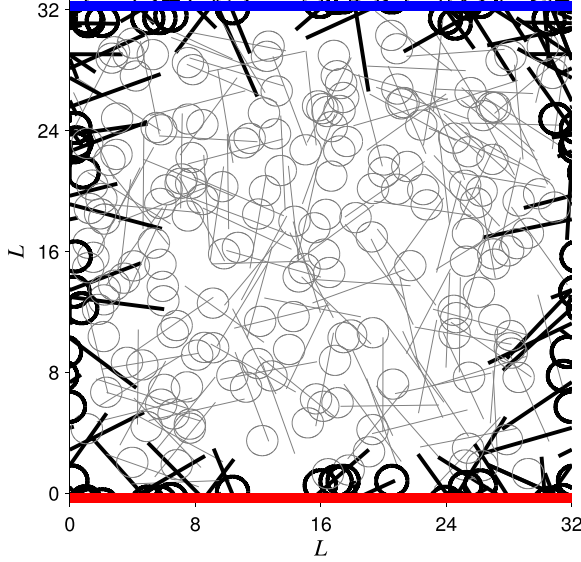


FIG. 1. Sample of randomly placed rings and sticks within a domain $L \times L$ with PBCs. All orientations of sticks are equiprobable. The domain size is $L = 32$. The ring radius is $r = 1$. The stick length is $l = 2\pi r$. The number of rings is $N_r = 200$. The number of sticks is $N_s = 200$. Busbars are shown as the thick lines at top and bottom of the system. The effect of the PBCs is demonstrated using black color.

this SLE does not present significant difficulties. We used the EIGEN library [36] to solve it.

We used domains of a fixed size $L = 32$, while the characteristic sizes of the fillers were $r = 1$ and $l = 2\pi r$. To efficiently determine the percolation threshold (occurrence of a percolation cluster that spans the system in a given direction), the union-find algorithm [37,38] was used. In our simulations, for the two limiting cases, when only one kind of filler is presented, $n_c = 0.373 \pm 0.004$ for rings, while $n_c = 5.641 \pm 0.025$ for sticks.

In our study, we concentrated on the experimental data published in Refs. [5,6]. Tables I and II suggest that in this case, the wire resistance $R_w \approx 125 \Omega$, i.e., of the same order of magnitude or less than the junction resistance R_j . Therefore, we focused our study on only two cases, viz., JDA and when the resistances of the wires and junctions are equal. Another limiting case when the wire resistance dominates over the junction resistance, considered, e.g., in Refs. [25,34], is hardly relevant for our system under consideration. In all our computations, we set $R_b = 0$.

The results of the computations presented in Sec. III were averaged over 10 independent runs. The error bars in the figures correspond to the standard deviation of the mean. When not shown explicitly, they are of the order of the marker size.

B. Analytical consideration

The probability of the intersection of any two rings is

$$P_r = 4\pi \left(\frac{r}{L}\right)^2 \quad (4)$$

(see, e.g., Refs. [26,39]). The probability that a given ring intersects exactly N other rings is described by the binomial distribution

$$\Pr(k = N) = \binom{N_r}{N} P_r^N (1 - P_r)^{N_r - 1 - N}. \quad (5)$$

The expected number of intersections is

$$\langle N_{rr} \rangle = P_r (N_r - 1) \approx 4\pi r^2 n_r, \quad (6)$$

since $N_r \gg 1$.

The probability of the intersection of any two sticks is

$$P_s = \frac{2}{\pi} \left(\frac{l}{L}\right)^2 \quad (7)$$

(see, e.g., Refs. [20,32,39]). The probability that a given stick intersects exactly N other sticks is described by the binomial distribution

$$\Pr(k = N) = \binom{N_s}{N} P_s^N (1 - P_s)^{N_s - 1 - N}. \quad (8)$$

The expected number of intersections is

$$\langle N_{ss} \rangle = P_s (N_s - 1) \approx \frac{2}{\pi} l^2 n_s, \quad (9)$$

since $N_s \gg 1$.

The probability that a stick and a ring have one point of intersection is

$$P_1 = \frac{r^2}{L^2} \begin{cases} 4(\arcsin z + z\sqrt{1-z^2}) & \text{if } z \leq 1 \\ 2\pi & \text{if } z > 1, \end{cases} \quad (10)$$

while the probability that a stick and a ring have two points of intersection is

$$P_2 = \frac{r^2}{L^2} \left[4z - \begin{cases} 2(\arcsin z + z\sqrt{1-z^2}) & \text{if } z \leq 1 \\ \pi & \text{if } z > 1 \end{cases} \right], \quad (11)$$

where

$$z = \frac{l}{2r} \quad (12)$$

(see Supplemental Material [40]). The probability of the intersection of a stick and a ring is

$$P_{rs} = P_1 + P_2 = \frac{r^2}{L^2} \left[4z + \begin{cases} 2(\arcsin z + z\sqrt{1-z^2}) & \text{if } z \leq 1 \\ \pi & \text{if } z > 1 \end{cases} \right]. \quad (13)$$

Thus, the expected number of intersections of a stick with a ring is

$$\langle k \rangle = \frac{P_1 + 2P_2}{P_{rs}} = \frac{8z}{4z + \psi}, \quad \text{where} \quad (14)$$

$$\psi = \begin{cases} 2(\arcsin z + z\sqrt{1-z^2}) & \text{if } 0 < z \leq 1 \\ \pi & \text{if } z > 1. \end{cases}$$

This quantity varies from $\langle k \rangle = 1$ when $z = 0$, through 1.6 when $z = \pi$ (i.e., $l = 2\pi r$), to 2 when $z \gg 1$ (Fig. 2).

The probability that a given ring intersects exactly N sticks is described by the binomial distribution

$$\Pr(k = N) = \binom{N_s}{N} P_{rs}^N (1 - P_{rs})^{N_s - 1 - N}. \quad (15)$$

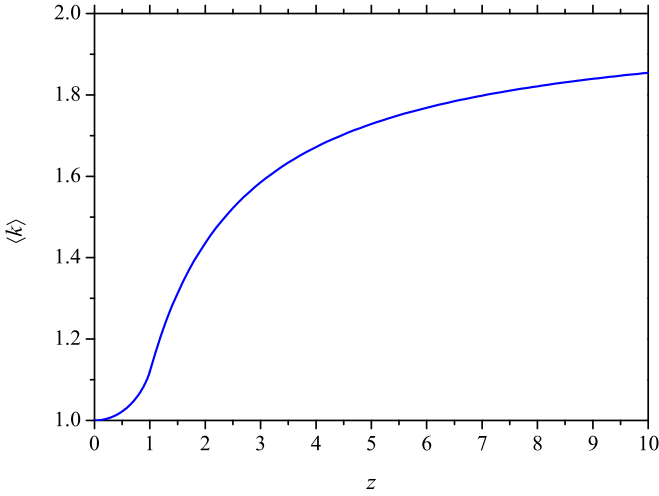


FIG. 2. Dependency of the average number of contacts between a stick and a ring, $\langle k \rangle$, on the relative length of the stick z [Eq. (14)].

The expected number of intersections is

$$\langle N_{rs} \rangle = P_{rs}(N_s - 1) \approx P_{rs}N_s, \quad (16)$$

since $N_s \gg 1$.

The probability that a given stick intersects exactly N rings is described by the binomial distribution

$$\Pr(k = N) = \binom{N_r}{N} P_{rs}^N (1 - P_{rs})^{N_r - 1 - N}. \quad (17)$$

The expected number of intersections is

$$\langle N_{sr} \rangle = P_{rs}(N_r - 1) \approx P_{rs}N_r, \quad (18)$$

since $N_r \gg 1$.

Thus, the expected number of contacts per ring is

$$\langle k_r \rangle = 2\langle N_{rr} \rangle + \langle k \rangle \langle N_{rs} \rangle, \quad (19)$$

while the expected number of contacts per stick is

$$\langle k_s \rangle = \langle N_{ss} \rangle + \langle k \rangle \langle N_{sr} \rangle. \quad (20)$$

For any allowed value of z ,

$$\langle k_r \rangle = 8\pi r^2 n_r + 4l n_s, \quad (21)$$

$$\langle k_s \rangle = \frac{2l^2}{\pi} n_s + 4l n_r. \quad (22)$$

When the number density of the conductive fillers is large enough, the variation of the electrical potential along the film is close to linear [24–27]. Only one conductive filler in the mean field produced by all the other fillers may be considered, rather than using a consideration of the whole system of fillers. This idea may be easily transferred to the case when the fillers of two different shapes are presented.

Consider a linear conductive wire (stick) in an external electric field. This stick is characterized by a resistance per unit length, ρ_w . Its lateral surface is supposed to be insulating, characterized by a leakage conductance per unit length,

$$G_s = \frac{R_j \langle k_s \rangle}{l}. \quad (23)$$

According to Ref. [24], the fraction of the electrical conductance, which is due to all sticks, is equal to

$$\sigma_s = \frac{n_s l}{2\rho_w} \left[1 - \sqrt{\frac{4}{\langle k_s \rangle \Delta}} \tanh \left(\sqrt{\frac{\langle k_s \rangle \Delta}{4}} \right) \right], \quad (24)$$

where

$$\Delta = \frac{\rho_w l}{R_j}. \quad (25)$$

Likewise, consider a circular conductive wire (ring) in an external electric field. This ring is characterized by a resistance per unit length, ρ_w . Its lateral surface is supposed to be insulating, characterized by a leakage conductance per unit length,

$$G_r = \frac{R_j \langle k_r \rangle}{2\pi r}. \quad (26)$$

According to Ref. [26], the fraction of the electrical conductance, which is due to all rings, is equal to

$$\sigma_r = \frac{\pi \lambda^2 r^3 n_r}{\rho_w (1 + \lambda^2 r^2)}, \quad (27)$$

where, in our case,

$$\lambda^2 = \frac{\rho_w}{R_j} \left[4r n_r + \frac{2l}{\pi} n_s \right]. \quad (28)$$

The electrical conductance of the system of conductive rings and sticks is

$$\sigma = \sigma_r + \sigma_s. \quad (29)$$

When $R_w \ll R_j$ (JDA),

$$\sigma_s \approx \frac{n_s l^2 \langle k_s \rangle}{24 R_j}. \quad (30)$$

For not very large values of the number density, when $\lambda^2 \ll 1$,

$$\sigma_r \approx \frac{\pi r^3 n_r}{R_j} \left[4r n_r + \frac{2l}{\pi} n_s \right]. \quad (31)$$

Thus,

$$\sigma \approx \frac{1}{R_j} \left[4\pi r^4 n_r^2 + 2l r^3 n_r n_s + \frac{n_s^2 l^4}{12\pi} + \frac{n_r n_s l^3 r}{6} \right]. \quad (32)$$

Let $n_s = xn$, $n_r = (1-x)n$; then,

$$\begin{aligned} \sigma &\approx \frac{n^2 r^4}{R_j} \\ &\times \left[4\pi(1-x)^2 + x(1-x) \left(\frac{2l}{r} + \frac{l^3}{6r^3} \right) + x^2 \frac{l^4}{12\pi r^4} \right]. \end{aligned} \quad (33)$$

In the particular case, when $l = 2\pi r$,

$$\sigma \approx \sigma_0 \left(1 - x + x \frac{\pi^2}{3} \right), \quad \sigma_0 = \frac{4\pi n^2 r^4}{R_j}. \quad (34)$$

Here, σ_0 corresponds to the electrical conductance of a pure ring system in the case of a JDA (31).

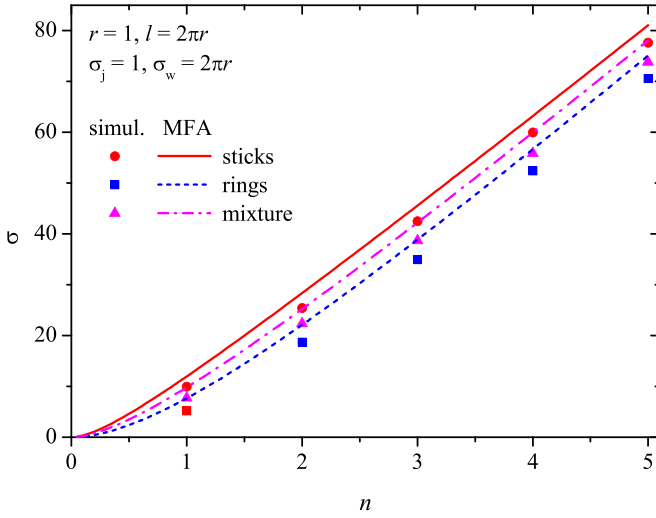


FIG. 3. Dependencies of the electrical conductance on the number density of fillers, $n = n_s + n_r$, when $n_r = 0$, $n_s = n_r$, and $n_s = 0$. The MFA predictions are shown as curves, while markers correspond to the simulations. Here, $l = 2\pi r$, $r = 1$, $R_j = 1$, and $\rho_w = (2\pi r)^{-1}$.

III. RESULTS

Figure 3 demonstrates the dependencies of the electrical conductance on the number density of the fillers for the three different proportions of rings and sticks (only rings, only sticks, and an equal parts mixture of rings and sticks). The wire resistance and the junction resistance are of the same order. For all used values of the number density, the MFA prediction slightly exceeds the simulated values of the electrical conductance.

Figure 4 presents the dependencies of the electrical conductance on the proportions of rings and sticks, x [$n_r = xn$ and $n_s = (1-x)n$], for the three different values of the number

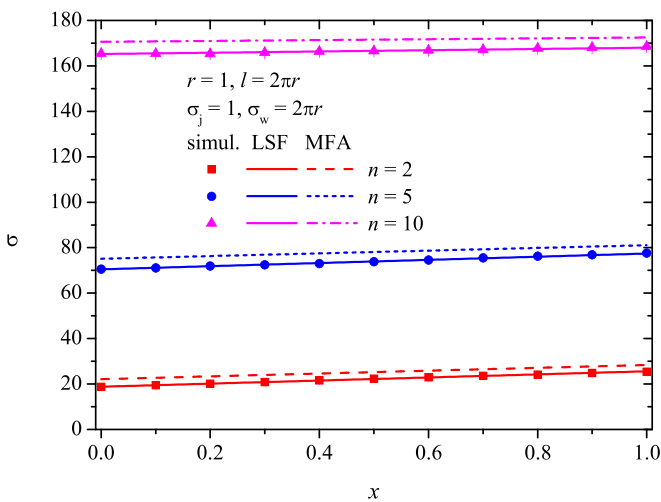


FIG. 4. Dependencies of the electrical conductance on the proportions of rings and sticks, x , for the three different values of the number density of fillers, $n_s = xn$ and $n_r = (1-x)n$, when $n = 2$, $n = 5$, and $n = 10$. MFA predictions and the least-squares fitting are shown as lines, while markers correspond to the simulations. Here, $l = 2\pi r$, $r = 1$, $R_j = 1$, and $\rho_w = (2\pi r)^{-1}$.

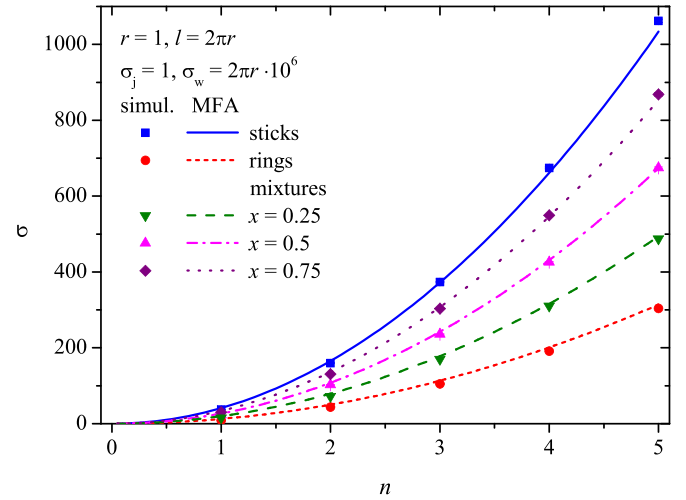


FIG. 5. Dependencies of the electrical conductance on the number density of fillers, $n = n_s + n_r$, when $n_r = 0$, $n_s = n_r$, $n_s = 3n_r$, $n_r = 3n_s$, and $n_s = 0$. MFA predictions are shown as curves, while markers correspond to the simulations. Here, $l = 2\pi r$, $r = 1$, $R_j = 1$, and $\rho_w = (2\pi r)^{-1}10^{-6}$.

density of fillers, when $n = 2$, $n = 5$, and $n = 10$. The MFA slightly overestimates the electrical conductance, as with the pure stick and pure ring systems [24–27]. When wire resistance and the junction resistance are of the same order, while $l = 2\pi r$, the electrical conductance is almost insensitive to the specific proportions of rings and sticks.

Figure 5 demonstrates the dependencies of the electrical conductance on the number density of fillers for the five different proportions of rings and sticks. The junction resistance

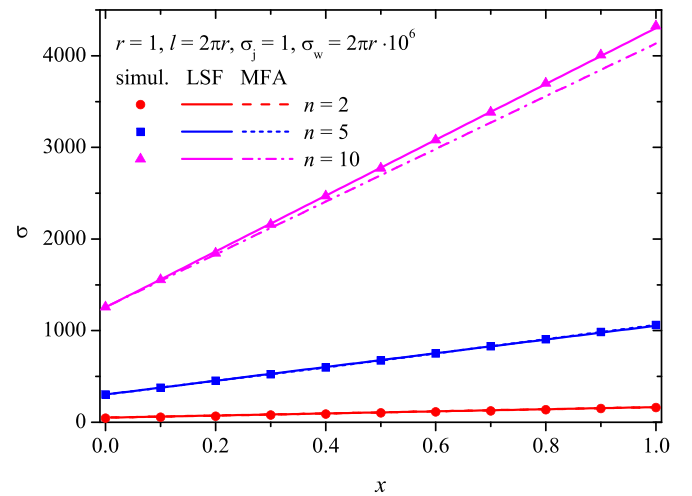


FIG. 6. Dependencies of the electrical conductance on the proportions of rings and sticks, x , for the three different values of the number density of fillers, $n_s = xn$ and $n_r = (1-x)n$, when $n = 2$, $n = 5$, and $n = 10$. MFA predictions and the least-squares fitting are shown as lines, while markers correspond to the simulations. For the two larger values of n , the difference between the MFA and LSF lines are not visually distinguishable. Here, $l = 2\pi r$, $r = 1$, $R_j = 1$, and $\rho_w = (2\pi r)^{-1}10^{-6}$.

TABLE III. Least-squares fitting of the dependencies of the electrical conductance on the proportions of rings and sticks, $\sigma = ax + b$. $l = 2\pi r$, $r = 1$, $R_j = 1$.

n	Slope (a)	Intercept (b)	Adj. R^2
$\rho_w = (2\pi r)^{-1}$			
2	6.79 ± 0.09	18.81 ± 0.05	0.99847
5	6.94 ± 0.15	70.47 ± 0.06	0.99542
10	2.76 ± 0.32	165.3 ± 0.1	0.88319
$\rho_w = (2\pi r)^{-1}10^{-6}$			
2	115	50	1
5	750 ± 3	302.9 ± 0.9	0.99981
10	3049 ± 10	1253.6 ± 2.5	0.99989

dominates over the wire resistance. MFA predictions and simulations are in good agreement.

Figure 6 presents the dependencies of the electrical conductance on the proportions of rings and sticks, x [$n_r = xn$ and $n_s = (1 - x)n$], for the three different values of the number density of fillers, viz., $n = 2$, $n = 5$, and $n = 10$, when the junction resistance dominates over the wire resistance. The dependencies are close to linear.

The coefficients of the least-squares fitting (LSF) of the dependencies of the electrical conductance on the proportions of rings and sticks are collected in Table III.

Figure 7 exhibits the dependencies of the normalized electrical conductance σ/σ_0 on the proportions of rings and sticks, x , for the three different values of the number density of fillers in the limiting case of JDA. The linear dependency predicted by an MFA (34) is consistent with the simulations.

Figure 8 demonstrates the dependencies of the electrical conductance on the proportions of rings and sticks, x , for

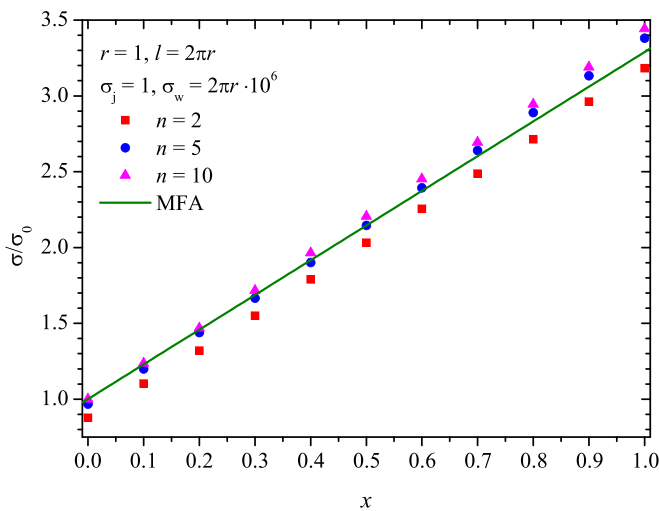


FIG. 7. Dependencies of the normalized electrical conductance on the proportions of rings and sticks, x , for the three different values of the number density of fillers, $n_s = xn$ and $n_r = (1 - x)n$, when $n = 2$, $n = 5$, and $n = 10$. The MFA predictions (34) are shown as a line, while markers correspond to the simulations. Here, $l = 2\pi r$, $r = 1$, $R_j = 1$, and $\rho_w = (2\pi r)^{-1}10^{-6}$.

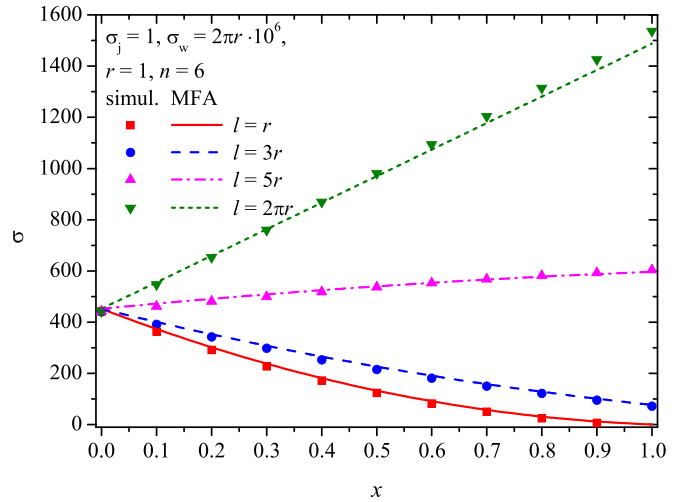


FIG. 8. Dependencies of the electrical conductance on the proportions of rings and sticks, x , for the fixed values of the number density of fillers and different values of l . MFA predictions are shown as curves, while markers correspond to the simulations. Here, $r = 1$, $R_j = 1$, and $\rho_w = (2\pi r)^{-1}10^{-6}$, $n = 6$.

the fixed values of the number density of fillers and different values of l , when the junction resistance dominates over the wire resistance (JDA). The MFA predictions (33) are shown as curves, while the markers correspond to the simulations.

Figure 9 demonstrates the dependencies of the electrical conductance on the relative stick length, z , for the fixed values of the number density of fillers and different values of x , when the junction resistance dominates over the wire resistance (JDA). The MFA predictions (33) are shown as curves, while the markers correspond to the simulations.

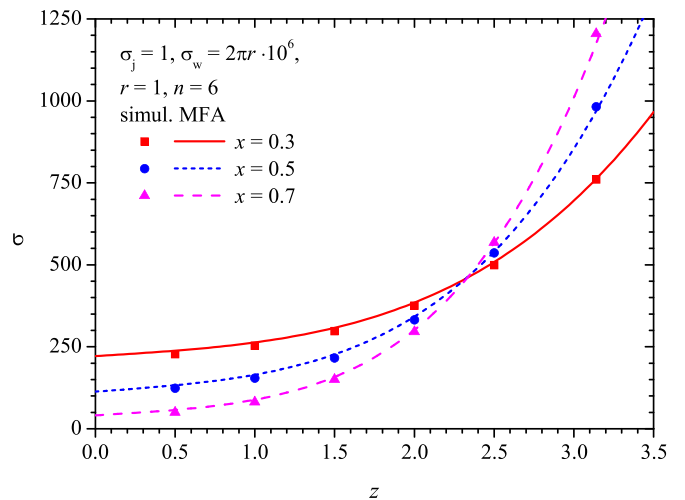


FIG. 9. Dependencies of the electrical conductance on the relative stick length, z , for the fixed values of the number density of fillers and different values of x . The MFA predictions are shown as curves, while the markers correspond to the simulations. Here, $r = 1$, $R_j = 1$, and $\rho_w = (2\pi r)^{-1}10^{-6}$, $n = 6$.

IV. CONCLUSION

The electrical conductance of 2D random percolating networks of zero-width metallic nanowires (a mixture of rings and sticks) has been studied using both a mean-field approximation and a computer simulation. We took into account the nanowire resistance per unit length and the junction (nanowire-nanowire contact) resistance (the so-called multinodal representation, MNR [16,22]). We derived the total electrical conductance of the nanowire-based networks as a function of their geometrical and physical parameters. Our MC simulations were focused on the case when the circumferences of the rings and the lengths of the wires were equal. Our MC simulations confirmed the MFA predictions. The electrical conductance of the network is almost insensitive to the proportions of rings and sticks when the wire resistance and the junction resistance are equal. When the junction resistance dominates over the wire resistance, a linear dependency of the electrical conductance of the network on the proportions of rings and sticks was observed. The dispersity of the physical parameters and sizes inevitably presented in any real-world system can hardly affect the main results of the MFA since only the mean values of all the quantities are important within the MFA. The effect of the dispersity on the results of the

simulation is expected to be only an increase in the standard deviation.

There are, at least, two obvious directions of further study. First, since real-world NWs are often bent, more realistic shapes of NWs should be considered instead of sticks. Although the percolative and electrical properties of bent and waved NWs have been studied [35,39,41–43], there are a number of open questions to be solved. In particular, a mixture of arcs of different curvature up to closed-up arcs (rings) has, to the best of our knowledge, not yet been studied. Second, direct comparison with experimental data is necessary. Such a comparison requires, simultaneously, data on the wire resistance, the junction resistance, the transparency, the sheet resistance, the geometrical parameters of both NWs and NRs, and the composition (NR to NW ratios) of the samples. However, direct measurements of the junction resistance are currently limited owing to the small number of teams working on these.

ACKNOWLEDGMENTS

We would like to acknowledge funding from the Foundation for the Advancement of Theoretical Physics and Mathematics “BASIS”, Grant No. 20-1-1-8-1. We thank I.V. Vodolazskaya for our fruitful discussions.

-
- [1] S. Huang, Y. Liu, F. Yang, Y. Wang, T. Yu, and D. Ma, Metal nanowires for transparent conductive electrodes in flexible chromatic devices: A review, *Environ. Chem. Lett.* **20**, 3005 (2022).
- [2] L. Zhou, X.-F. Fu, L. Yu, X. Zhang, X.-F. Yu, and Z.-H. Hao, Crystal structure and optical properties of silver nanorings, *Appl. Phys. Lett.* **94**, 153102 (2009).
- [3] Y. Zhan, Y. Lu, C. Peng, and J. Lou, Solvothermal synthesis and mechanical characterization of single crystalline copper nanorings, *J. Cryst. Growth* **325**, 76 (2011).
- [4] Z. Yin, S. K. Song, D.-J. You, Y. Ko, S. Cho, J. Yoo, S. Y. Park, Y. Piao, S. T. Chang, and Y. S. Kim, Novel synthesis, coating, and networking of curved copper nanowires for flexible transparent conductive electrodes, *Small* **11**, 4576 (2015).
- [5] M.-R. Azani and A. Hassanpour, Silver nanorings: New generation of transparent conductive films, *Chem. Eur. J.* **24**, 19195 (2018).
- [6] M.-R. Azani, A. Hassanpour, Y. Y. Tarasevich, I. V. Vodolazskaya, and A. V. Eserkepov, Transparent electrodes with nanorings: A computational point of view, *J. Appl. Phys.* **125**, 234903 (2019).
- [7] Z. Li, D. Guo, P. Xiao, J. Chen, H. Ning, Y. Wang, X. Zhang, X. Fu, R. Yao, and J. Peng, Silver nanorings fabricated by glycerol-based cosolvent polyol method, *Micromachines* **11**, 236 (2020).
- [8] C. Feng, Z. Zhong, S. Lin, Y. Liu, and J. Hu, Synthesis of silver nanorings via a facile one-pot method, *Inorg. Chem. Commun.* **130**, 108703 (2021).
- [9] H. Ning, Z. Li, J. Chen, X. Fu, Z. Fang, R. Yao, J. Huang, H. Ren, X. Cao, and J. Peng, Synthesis of silver nanorings through a glycerol-base polyol method, *Mol. Cryst. Liq. Cryst.* **733**, 39 (2022).
- [10] A. Bid, A. Bora, and A. K. Raychaudhuri, Temperature dependence of the resistance of metallic nanowires of diameter ≥ 15 nm: Applicability of Bloch-Grüneisen theorem, *Phys. Rev. B* **74**, 035426 (2006).
- [11] R. A. Serway and J. W. Jewett, *Principles of Physics*, 5th ed., Vol. 1 (Brooks/Cole Cengage Learning, Boston, MA, 2013), p. 592.
- [12] Y. Zhao, M. L. Fitzgerald, Y. Tao, Z. Pan, G. Sauti, D. Xu, Y.-Q. Xu, and D. Li, Electrical and thermal transport through silver nanowires and their contacts: Effects of elastic stiffening, *Nano Lett.* **20**, 7389 (2020).
- [13] D. Kojda, R. Mitdank, M. Handwerg, A. Mogilatenko, M. Albrecht, Z. Wang, J. Ruhhammer, M. Kroener, P. Woias, and S. F. Fischer, Temperature-dependent thermoelectric properties of individual silver nanowires, *Phys. Rev. B* **91**, 024302 (2015).
- [14] J. Wang, Z. Wu, C. Mao, Y. Zhao, J. Yang, and Y. Chen, Effect of electrical contact resistance on measurement of thermal conductivity and Wiedemann-Franz law for individual metallic nanowires, *Sci. Rep.* **8**, 4862 (2018).
- [15] A. T. Bellew, H. G. Manning, C. Gomes da Rocha, M. S. Ferreira, and J. J. Boland, Resistance of single Ag nanowire junctions and their role in the conductivity of nanowire networks, *ACS Nano* **9**, 11422 (2015).
- [16] C. Gomes da Rocha, H. G. Manning, C. O’Callaghan, C. Ritter, A. T. Bellew, J. J. Boland, and M. S. Ferreira, Ultimate conductivity performance in metallic nanowire networks, *Nanoscale* **7**, 13011 (2015).
- [17] F. Selzer, C. Floresca, D. Knepp, L. Bormann, C. Sachse, N. Weiß, A. Eychmüller, A. Amassian, L. Müller-Meskamp, and K. Leo, Electrical limit of silver nanowire electrodes: Direct measurement of the nanowire junction resistance, *Appl. Phys. Lett.* **108**, 163302 (2016).

- [18] Z. Cheng, L. Liu, S. Xu, M. Lu, and X. Wang, Temperature dependence of electrical and thermal conduction in single silver nanowire, *Sci. Rep.* **5**, 10718 (2015).
- [19] N. Charvin, J. Resende, D. T. Papanastasiou, D. Muñoz-Rojas, C. Jiménez, A. Nourdine, D. Bellet, and L. Flandin, Dynamic degradation of metallic nanowire networks under electrical stress: a comparison between experiments and simulations, *Nanoscale Adv.* **3**, 675 (2021).
- [20] D. Kim and J. Nam, Systematic analysis for electrical conductivity of network of conducting rods by Kirchhoff's laws and block matrices, *J. Appl. Phys.* **124**, 215104 (2018).
- [21] C. Forró, L. Demkó, S. Weydert, J. Vörös, and K. Tybrandt, Predictive model for the electrical transport within nanowire networks, *ACS Nano* **12**, 11080 (2018).
- [22] H. G. Manning, C. Gomes da Rocha, C. O'Callaghan, M. S. Ferreira, and J. J. Boland, The electro-optical performance of silver nanowire networks, *Sci. Rep.* **9**, 11550 (2019).
- [23] D. Kim and J. Nam, Electrical conductivity analysis for networks of conducting rods using a block matrix approach: A case study under junction resistance dominant assumption, *J. Phys. Chem. C* **124**, 986 (2020).
- [24] Y. Y. Tarasevich, I. V. Vodolazskaya, and A. V. Eserkepov, Electrical conductivity of random metallic nanowire networks: an analytical consideration along with computer simulation, *Phys. Chem. Chem. Phys.* **24**, 11812 (2022).
- [25] Y. Y. Tarasevich, A. V. Eserkepov, and I. V. Vodolazskaya, Electrical conductivity of nanorod-based transparent electrodes: Comparison of mean-field approaches, *Phys. Rev. E* **105**, 044129 (2022).
- [26] Y. Y. Tarasevich, A. V. Eserkepov, and I. V. Vodolazskaya, Electrical conductivity of nanoring-based transparent conductive films: A mean-field approach, *J. Appl. Phys.* **130**, 244302 (2021).
- [27] Y. Y. Tarasevich, A. V. Eserkepov, and I. V. Vodolazskaya, Random 2D nanowire networks: Finite-size effect and the effect of busbar/nanowire contact resistance on their electrical conductivity, *J. Appl. Phys.* **132**, 125105 (2022).
- [28] M. Žeželj and I. Stanković, From percolating to dense random stick networks: Conductivity model investigation, *Phys. Rev. B* **86**, 134202 (2012).
- [29] A. Kumar, N. S. Vidhyadhiraja, and G. U. Kulkarni, Current distribution in conducting nanowire networks, *J. Appl. Phys.* **122**, 045101 (2017).
- [30] D. Kim and J. Nam, Analyzing conducting rod networks using centrality, *Electrochim. Acta* **370**, 137725 (2021).
- [31] R. K. Daniels and S. A. Brown, Nanowire networks: How does small-world character evolve with dimensionality?, *Nanoscale Horiz.* **6**, 482 (2021).
- [32] C. O'Callaghan, C. Gomes da Rocha, H. G. Manning, J. J. Boland, and M. S. Ferreira, Effective medium theory for the conductivity of disordered metallic nanowire networks, *Phys. Chem. Chem. Phys.* **18**, 27564 (2016).
- [33] X. Ni, C. Hui, N. Su, W. Jiang, and F. Liu, Monte Carlo simulations of electrical percolation in multicomponent thin films with nanofillers, *Nanotechnology* **29**, 075401 (2018).
- [34] J. Hicks, A. Behnam, and A. Ural, Resistivity in percolation networks of one-dimensional elements with a length distribution, *Phys. Rev. E* **79**, 012102 (2009).
- [35] J. Hicks, J. Li, C. Ying, and A. Ural, Effect of nanowire curviness on the percolation resistivity of transparent, conductive metal nanowire networks, *J. Appl. Phys.* **123**, 204309 (2018).
- [36] G. Guennebaud, B. Jacob *et al.*, Eigen v3, <http://eigen.tuxfamily.org> (unpublished).
- [37] M. E. J. Newman and R. M. Ziff, Efficient Monte Carlo Algorithm and High-Precision Results for Percolation, *Phys. Rev. Lett.* **85**, 4104 (2000).
- [38] M. E. J. Newman and R. M. Ziff, Fast Monte Carlo algorithm for site or bond percolation, *Phys. Rev. E* **64**, 016706 (2001).
- [39] Y. B. Yi, L. Berhan, and A. M. Sastry, Statistical geometry of random fibrous networks, revisited: Waviness, dimensionality, and percolation, *J. Appl. Phys.* **96**, 1318 (2004).
- [40] See Supplemental Material at <http://link.aps.org/supplemental/10.1103/PhysRevE.107.034105> for the derivation of these probabilities.
- [41] D. P. Langley, M. Lagrange, N. D. Nguyen, and D. Bellet, Percolation in networks of 1-dimensional objects: Comparison between Monte Carlo simulations and experimental observations, *Nanoscale Horiz.* **3**, 545 (2018).
- [42] K. Esteki, H. G. Manning, E. Sheerin, M. S. Ferreira, J. J. Boland, and C. Gomes da Rocha, Tuning the electro-optical properties of nanowire networks, *Nanoscale* **13**, 15369 (2021).
- [43] J. Lee and J. Nam, Percolation threshold of curved linear objects, *Phys. Rev. E* **103**, 012126 (2021).